Accelerating Blind Deconvolution: A Pre-processing Approach for Point Spread Function Size Estimation

Yasser Elmi Sola

Department of Computer Engineering, Sab.C., Islamic Azad University, Sabzevar, Iran,Yasser.elmi@iau.ac.ir

Abstract

Existing approaches in blind image deblurring often take the blur kernel size as a manual parameter, and when this parameter is not set correctly, it can lead to significant errors in the estimated kernel. Given that multiple other parameters also influence each deblurring operation with a specified kernel size, manually determining the kernel size is a tedious task and often results in trial and error for the user to find the best size. Therefore, proposing an automatic method for the initial estimation of the kernel size can be beneficial as a pre-processing step in blind deblurring operations. In this paper, we propose a new approach for the automatic estimation of the kernel size. In this approach, we utilize the quality curve of deblurred images with kernels of different sizes to find the optimal point. In this process, a blind deblurring method is employed to deblur the image, and a no-reference quality assessment metric is used to evaluate the quality of the deblurred images. The implementation results indicate that the proposed method provides more accurate estimates compared to existing methods, such that the mean absolute error of the estimates in the proposed method is 78% better than that of the best existing methods.

Keywords: Blur kernel, Point spread function, Blind deblurring, Image quality assessment, Interpolation
Article history: Received 2025/07/19; Revised 2025/08/01, Accepted 2025/08/08, Article Type: Research paper

https://doi.org/10.82234/IJSEE.2025.1212400

1. Introduction

Image blurriness due to hand tremors is one of the problems faced by handheld cameras. Image blurriness can be modelled as the convolution of the original sharp image with the impulse response of the imaging system, known as the Point Spread Function (PSF), as follows:

$$B = k \otimes I + n \quad (1)$$

where B is the blurred image received by the camera, k is the blur kernel, I is the original sharp image, n is noise, and the operator $\otimes$ denotes convolution. The goal of blind deconvolution is to compute I and k using B*B*, which is a severely ill-posed problem due to the multiplicity of possible responses [1]. Blind deconvolution has been extensively studied in recent years, and various methods have been proposed to address this issue [2-7]. These methods utilize convolutional neural networks, deep learning [8-12], advanced mathematical models, iterative methods, and metaheuristic algorithms to solve the problem. One significant limitation of all existing deblurring methods is that they require an estimated size of the blur kernel as an input parameter [13]. Additionally, these methods are sensitive to the kernel size, and even minor variations can lead to significant impacts on the results. An example of the effect of an incorrect initial estimate of the blur kernel is illustrated in Figure 1. Limited methods have been proposed for estimating the size of the blur kernel. Liu et al. [14] used an autocorrelation map of the image gradient, which reflects information regarding image blurriness, and employed an enhanced autocorrelation map to extract information related to image blurriness while reducing the adverse effects of structural edges. Li et al. [16] utilized a convolutional neural network (CNN) in their proposed method, where a neural network was trained on a dataset of blurred images. Their results indicate that the estimates from Li et al. are more accurate than those from Liu et al.; however, a major drawback of their method is the dependence of the neural network on the training dataset. In this paper, a method is proposed that operates based on

estimating the maximum point on the quality curve of the deblurred images. The most important feature of this method is its flexibility and the capability to incorporate various methods seamlessly. Given that in the proposed method, the estimation of the blur kernel size is performed completely automatically and does not require actual deblurring, the proposed approach can be considered as a pre-processing step for most existing image deblurring methods.

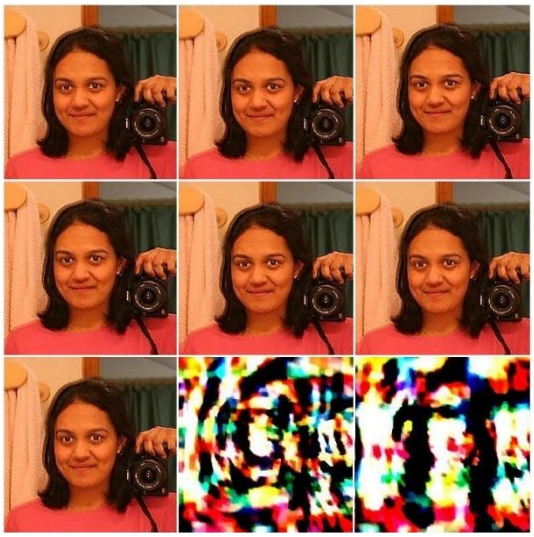

Fig. 1. Deblurring using kernels of varying sizes from 11×11 to 91×91

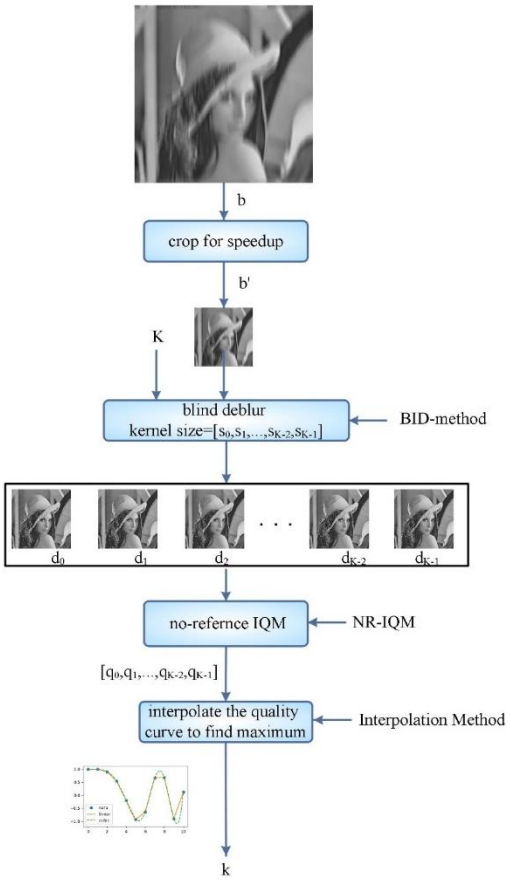

Fig. 2. Overall schematic of the proposed method

2. Proposed Method

In this paper, a new approach for the automatic estimation of the appropriate kernel size for blind deconvolution is presented. The key element in the proposed method is the interpolation of the quality curve of the deblurred images concerning the kernel size. In the first step, a portion of the original blurred image is cropped. This operation is performed to reduce computational load and increase execution speed. During implementation, if execution time is not critical, the size of the cropped area can be increased for higher accuracy, or this step can be entirely omitted. After cropping the image and selecting a small region from it, K initial random values are generated as the kernel size, and this set of values $k_s = \{S_0, S_1, \dots, S_{k-1}\}$ is used as the kernel size in blind deconvolution. The quality of deblurring is then computed for these K images using a no-reference quality assessment metric, which forms K points on the image quality curve as a function of the kernel size. To find the optimal kernel size, this curve is interpolated, and its maximum point is calculated. Figure 2 summarizes how the method operates.

In our implementation, 64×64 patches were selected in the first step, and this selection can be increased based on the required accuracy. In the best case, with more time spent, this step can even be omitted. Based on the experiments conducted, K=9 was chosen.

As shown in Figure 3, the three stages of this algorithm can be executed flexibly and with various methods. In other words, during the blind deconvolution stage, the no-reference image quality assessment stage, and the interpolation stage, a wide range of existing methods and their combinations can be utilized. Although simulation results indicate that some combinations lead to more accurate outputs, which will be discussed further. In our implementation for blind deconvolution, we used the algorithm of Sci et al. [4], the no-reference image quality assessors SI [15], OQM, BRISQUE, and NIQE [17,18,19], and the Spline method for interpolation. Figure 3 displays the initial blurred image, the cropped section of the initial blurred image from the first stage of the algorithm, along with the deblurred images obtained using the algorithm of Krishnan et al. [20] with 9 random kernel sizes. The quality of the nine deblurred images was assessed using the no-reference image quality assessor SI, and the quality curve of the deblurred images as a function of the kernel size was plotted using the interpolation method. As seen in this figure, the local and global maxima of the images are at points 43 and 77, respectively,

suggesting that the user should conduct tests to find the best deblurred image around these points.

In recent studies on image quality assessment, it has become evident that the curves generated by different quality metrics, specifically Structural Similarity Index (SI) [15], Blind/Referenceless Image Spatial Quality Evaluator (BRIQUE) [16], and Information Loss Metric for No-Reference Image Quality Evaluation (IL-NIQE) [19], show a significant degree of convergence. This convergence suggests that these metrics, despite their distinct methodologies and theoretical foundations, are effectively capturing similar perceptual quality attributes in images. The SI metric, known for its ability to assess structural information, aligns closely with the perceptual quality evaluations provided by BRIQUE and IL-NIQE, which focus on the spatial and information loss characteristics of images.

The evaluation curves for SI, BRIQUE, and IL-NIQE demonstrate that as the perceived quality of an image increases, the scores from these metrics tend to rise in a correlated manner. This correlation indicates that all three metrics are sensitive to the same underlying quality factors, such as contrast, noise, and detail preservation. For example, when analyzing a set of distorted images, the consistent upward trend in the quality scores across these metrics reinforces the idea that they are measuring similar aspects of image fidelity. Such behavior is crucial for researchers and practitioners who rely on these metrics for objective quality assessment.

Moreover, the convergence of these evaluation curves has practical implications for the development and refinement of image processing algorithms. By validating that SI, BRIQUE, and IL-NIQE yield comparable quality assessments, researchers can confidently utilize any of these metrics in their evaluations, knowing that they will likely produce consistent results. This consistency not only streamlines the evaluation process but also enhances the reliability of comparative studies in image processing, leading to improved methodologies and outcomes in various applications, from medical imaging to multimedia content delivery.

3. Simulation Results

The simulation was conducted in four sections. In the first stage, a suitable combination of the components constituting the overall method, including the deblurring method, the no-reference quality assessment metric, and the interpolation method, was determined. In the second stage, the kernel size estimation was performed on artificially blurred images, and in the third stage, this estimation was applied to naturally blurred images.

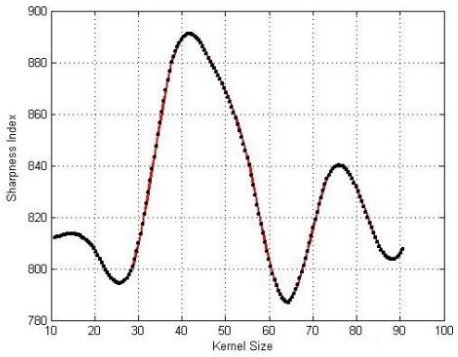

Fig. 3. Interpolation of the quality curve for the deblurred image using the SI metric.

A) Choosing the Suitable Components

Considering that the proposed method can utilize a diverse combination of deblurring methods, image quality assessment metrics, and various interpolation methods without compromising the overall approach, in this implementation, we used the method of Elmi et al. [4] for the blind deconvolution phase, the no-reference quality assessors SI for the image quality assessment phase, and the Spline method for the interpolation phase. The combination of the deblurring method [4] and the SI quality assessor was chosen because this deblurring method employs a pyramid of image edges at different scales as a prior deconvolution, thus allowing the SI assessor to be more suitably employed for plotting the image quality curve as a function of the kernel size. Table 1 shows the quality of deblurred images with kernel sizes ranging from 11×11 to 101×101, assessed using the image quality assessors SI, BRISQUE, Overall Quality Metric, and IL-NIQE. This example illustrates that the extrema of these curves, displayed in Figure 4, do not align with each other. The results indicate that the highest alignment of the main kernel size occurs using the SI assessor.

Figure 4 illustrates that the proposed method yields varying results based on the quality assessment metric employed. Experiments conducted on multiple kernels demonstrated that the SI quality assessment metric, which operates by measuring the sharpness of image edges, produces superior results.

B) Experiments on Artificially Blurred Images

To evaluate the accuracy of the kernel size estimation, a set of four images was utilized, sourced from the dataset presented by Sun and Hays [21], along with a collection of four blur kernels of different shapes. The initial images, kernels, and their corresponding blurred images are displayed in Figure 5. In this image set, care was taken to include various types of images in terms of detail, texture, edges, and lighting range. For the kernel set, kernels

with different shapes were considered, including linear, spreading, one-sided, two-sided, regular, and irregular forms. Tables 2, 3, and 4 present the estimated results obtained using the proposed algorithm for each kernel, compared to the original values.

In Tables 3 to 5, we observe the outputs of the proposed method. These values can serve as starting points for testing in blind deconvolution algorithms. As seen in these tables, three values are suggested to the user for each method, and this number can be adjusted to be more or less. The results indicate that all three methods provided suitable estimates. For a more precise comparison, Table 6 displays the Mean Squared Error (MSE) for the best estimates from each of the three evaluators. The results in Table 6 show that when using blurred images from the dataset with the blur kernels shown in Figure 5, the BRISQUE evaluator provided more accurate results compared to the other evaluators.

Table.1.
Quality assessment curves for deblurred images with kernels sized from 11×11 to 101×101.

Kernel Size	*SI*	*OQM*	*BRISQUE*	*IL-NIQE*
11×11	362	-0.48	28.48	42.48
21×21	389	-0.47	28.22	42.01
31×31	352	-0.55	32.95	40.27
41×41	359	-0.51	31.99	40.83
51×51	357	-0.52	32.14	40.68
61×61	376	-0.53	31.59	40.37
71×71	376	-0.55	29.31	41.40
81×81	390	-0.49	30.91	39.72
91×91	380	-0.49	30.97	39.81
101×101	379	-0.47	28.89	41.61

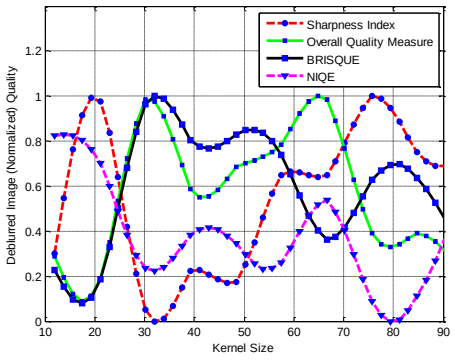

Fig. 4. Interpolation of the quality assessment curve for the image.

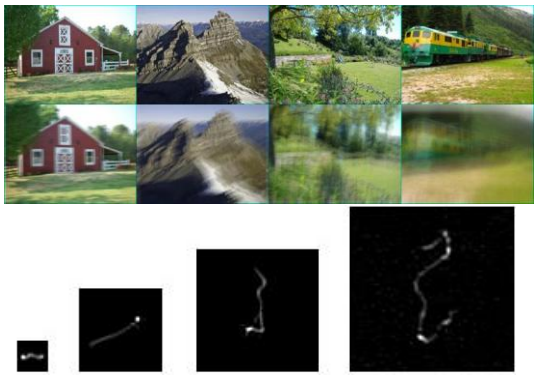

Fig. 5. Blurred images with kernels of different sizes alongside the original sharp image.

Table.2.
Estimated results obtained using the proposed algorithm with the SI evaluator.

	SI	*Original Size*
Image #1	25-31-46	19×19
Image #2	47-61-105	51×51
Image #3	39-56-79	75×75
Image #4	77-95-119	101×101

Table.3.
Estimated results obtained using the proposed algorithm with the IL-NIQE evaluator.

	IL-NIQE	*Original Size*
Image #1	19-58-86	19×19
Image #2	45-65-85	51×51
Image #3	49-77-89	75×75
Image #4	95-107-147	101×101

Table.4.
Estimated results obtained using the proposed algorithm with the BRISQUE evaluator.

	BRISQUE	*Original Size*
Image #1	19-62-90	19×19
Image #2	41-49-65	51×51
Image #3	49-63-79	75×75
Image #4	25-103-137	101×101

Table.5.
Mean Squared Error of the estimates from the proposed method using three different IQM.

	SI	*IL-NIQE*	*BRISQUE*
MSE	26	19	6

To better evaluate the proposed method, the results of the proposed approach were compared with the estimates from Liu et al. [14] and Li et al. [16]. Liu et al. estimates the blur kernel size using autocorrelation map, while Li et al. employs

convolutional neural networks (CNNs) for this task. The dataset used to assess the performance of the methods is the Levin image dataset [22], which consists of 32 blurred (non-square) images. This dataset consists of 32 images generated by applying 8 point spread functions to 4 sharp images. The results of the Autocorrelation map and CNN methods, alongside the estimates from the proposed method, are presented in Table 6, and the mean squared errors of the methods listed in Table 7 are shown in Table 7. The results in Tables 6 and 7 indicate that the mean squared error and mean absolute e of the proposed method is approximately 78% better than that of the other methods.

Table.6.
Comparison of the proposed method's results with the results of [14] and [16].

PSF	*Original Automap*	*Modified Automap*	*CNN*	*Ours*	*Truth*
1	49	20	16	17	15
	46	17	14	17	10
2	50	20	15	15	16
	35	20	17	15	14
3	37	15	13	11	11
	36	16	11	11	10
4	52	29	26	25	24
	47	36	25	25	23
5	35	18	12	13	12
	42	18	12	13	12
6	45	27	26	19	20
	42	27	27	19	17
7	49	30	28	23	22
	38	25	22	23	17
8	51	40	20	19	21
	37	26	18	19	17

Table.7.
Mean squared error and mean absolute error in the proposed method and methods [14] and [16].

	Original Automap	*Modified Automap*	*CNN*	*Ours*
MSE	11556	945	103	33
MAE	26.8	7.6	2.5	1.4

4. Conclusion

In this paper, we addressed the challenges present in the image deblurring process, one of the most significant issues being the reliance on the blur kernel size as an input parameter. Common methods typically require manual adjustment of this parameter, which can lead to substantial errors in kernel estimation and, consequently, a decline in image quality. Therefore, an automatic method for estimating the kernel size was proposed as a preprocessing step in blind deconvolution operations. This novel approach effectively estimates the appropriate kernel size using the quality curve of deblurred images and no-reference quality assessment, allowing users to achieve better results without the need for trial and error.

Simulation results demonstrated that the proposed method can estimate the kernel size with reasonable accuracy and offers high flexibility. This method can be considered a preprocessing step for other deblurring techniques and is particularly effective in scenarios where reference images are unavailable. Ultimately, the quality assessment of deblurred images using various metrics showed that the proposed method can significantly enhance image quality and serve as an efficient tool in the field of image processing.

References

[1] A. Mosleh, Y. E. Sola, F. Zargari, E. Onzon, and J. P. Langlois, "Explicit ringing removal in image deblurring," *IEEE Trans. Image Process.*, vol. 27, no. 2, pp. 580-593, 2017.

[2] J. Pan, D. Sun, H. Pfister, and M.-H. Yang, Eds., "Blind image deblurring using dark channel prior," in *Proc. IEEE Conf. Comput. Vis. Pattern Recognit.*, 2016.

[3] L. Chen, F. Fang, T. Wang, and G. Zhang, Eds., "Blind image deblurring with local maximum gradient prior," in *Proc. IEEE/CVF Conf. Comput. Vis. Pattern Recognit.*, 2019.

[4] Y. E. Sola, F. Zargari, and A. M. Rahmani, "Blind image deblurring based on multi-resolution ringing removal," *Signal Process.*, vol. 154, pp. 250-259, 2019.

[5] B. Luo, Z. Cheng, L. Xu, G. Zhang, and H. Li, "Blind image deblurring via superpixel segmentation prior," *IEEE Trans. Circuits Syst. Video Technol.*, vol. 32, no. 3, pp. 1467-1482, 2021.

[6] Q. Zhao, H. Wang, Z. Yue, and D. Meng, "A deep variational Bayesian framework for blind image deblurring," *Knowl.-Based Syst.*, vol. 249, p. 109008, 2022.

[7] A. Eqtedaei and A. Ahmadyfard, "Coarse-to-fine blind image deblurring based on K-means clustering," *The Visual Comput.*, vol. 40, no. 1, pp. 333-344, 2024.

[8] L. Chen, X. Tian, S. Xiong, Y. Lei, and C. Ren, "Unsupervised blind image deblurring based on self-enhancement," in *Proc. IEEE/CVF Conf. Computer Vision and Pattern Recognition*, 2024, pp. 25691-25700.

[9] J. Peng, B. Luo, L. Xu, J. Yang, C. Zhang, and Z. Pei, "Blind image deblurring via minimizing similarity between fuzzy sets on image pixels," *IEEE Trans. Circuits Syst. Video Technol.*, 2024.

[10] Z. Guo, Z. Zhang, W. Yan, Z. Wu, Z. Xu, H. Chen, Y. Ji, C. Wang, J. Lai, and Z. Li, "Gradient domain model-driven algorithm unfolding network for blind image deblurring," *Neural Networks*, vol. 132, pp. 107683, 2025.

[11] Y. Li, M. Tofighi, J. Geng, V. Monga, and Y. C. Eldar, "Efficient and interpretable deep blind image deblurring via algorithm unrolling," *IEEE Trans. Comput. Imaging*, vol. 6, no. 4, pp. 666-681, 2020.

[12] R. Yan and L. Shao, "Blind image blur estimation via deep learning," *IEEE Trans. Image Process.*, vol. 25, no. 4, pp. 1910-1921, 2016.

[13] Y. Elmi, F. Zargari, and A. M. Rahmani, "Iterative approach for parametric PSF estimation," *Multimedia Tools Appl.*, vol. 79, pp. 29433-29450, 2020.

[14] S. Liu, H. Wang, J. Wang, S. Cho, and C. Pan, "Automatic blur-kernel-size estimation for motion deblurring," *The Visual Comput.*, vol. 31, pp. 733-746, 2015.

[15] Z. Wang, A. C. Bovik, H. R. Sheikh, and E. P. Simoncelli, "Image quality assessment: From error visibility to structural similarity," *IEEE Transactions on Image Processing*, vol. 13, no. 4, pp. 600-612, Apr. 2004.

[16] L. Li, N. Sang, L. Yan, and C. Gao, "Motion-blur kernel size estimation via learning a convolutional neural network," *Pattern Recognit. Lett.*, vol. 119, pp. 86-93, 2019.

[17] A. Mittal, R. Soundararajan, and A. C. Bovik, "Making a 'completely blind' image quality analyzer," *IEEE Signal Process. Lett.*, vol. 20, no. 3, pp. 209-212, 2012.

[18] A. Mittal, A. K. Moorthy, and A. C. Bovik, "No-reference image quality assessment in the spatial domain," *IEEE Trans. Image Process.*, vol. 21, no. 12, pp. 4695-4708, 2012.

[19] H. R. Sheikh and A. C. Bovik, "Image Information and Visual Quality," *IEEE Transactions on Image Processing*, vol. 15, no. 2, pp. 430-444, Feb. 2006.

[20] D. Krishnan, T. Tay, and R. Fergus, Eds., "Blind deconvolution using a normalized sparsity measure," in *CVPR*, 2011, pp. 1-8.

[21] L. Sun and J. Hays, Eds., "Super-resolution from internet-scale scene matching," in *2012 IEEE Int. Conf. Comput. Photogr. (ICCP)*, 2012, pp. 1-8.

[22] A. Levin, Y. Weiss, F. Durand, and W. T. Freeman, "Understanding and evaluating blind deconvolution algorithms," in *2009 IEEE Conf. Computer Vision and Pattern Recognition*, 2009, pp. 1964-1971.